

New Physics backgrounds to the $H \rightarrow WW$ search at the LHC?

B. FEIGL^{1*}, H. RZEHA^{2†‡} AND D. ZEPPENFELD^{1§}

¹Institut für Theoretische Physik, Karlsruher Institut für Technologie
D-76128 Karlsruhe, Germany

² CERN, PH-TH, 1211 Geneva 23, Switzerland

Abstract

The searches for $H \rightarrow WW$ events at the LHC use data driven techniques for estimating the $q\bar{q} \rightarrow WW$ background, by normalizing the background cross section to data in a control region. We investigate the possibility that new physics sources which mainly contribute to the control region lead to an overestimate of Standard Model backgrounds to the Higgs boson signal and, thus, to an underestimate of the $H \rightarrow WW$ signal. A supersymmetric scenario with heavy squarks and gluinos but charginos in the 200 to 300 GeV region and somewhat lighter sleptons can lead to such a situation.

*email: bastian.feigl @ kit.edu

†On leave from: Albert-Ludwigs-Universität Freiburg, Physikalisches Institut, Freiburg, Germany.

‡email: heidi.rzehak @ cern.ch

§email: dieter.zeppenfeld @ kit.edu

1 Introduction

Among the Higgs search channels at the LHC, the decay into weak boson pairs is particularly important, because the tree level couplings of the Higgs boson to WW and ZZ allow to positively identify a scalar state as being associated with the vacuum expectation value which breaks the electroweak gauge symmetry. A Higgs boson produced via gluon fusion with subsequent decay into leptonically decaying W bosons is especially searched for, at the present time, because this channel is expected to produce the largest sample of $H \rightarrow VV$ events at the LHC. However, for a Higgs boson mass around 125 GeV, it does suffer from substantial backgrounds, the dominant one being $q\bar{q} \rightarrow W^+W^-$, followed by leptonic decay of the W bosons. In the present experimental analyses, this contribution to the background is estimated with data driven methods [1–3]. A control region of the phase space, namely events at large dilepton invariant mass $m_{\ell\ell}$, is defined where no signal events are to be expected. The size of the background is measured in this control region and the corresponding value in the signal region, at small $m_{\ell\ell}$, is then extrapolated using the shape of the distribution determined by a Monte Carlo simulation for Standard Model (SM) W pair production.

In this paper we investigate whether new physics contributions can seriously compromise this data driven background determination. Specifically, can new physics events, which typically are hard and thus tend to preferentially populate the large $m_{\ell\ell}$ region, significantly enhance the size of the background measured in the control region, while contributing relatively less than the SM W pair production to the signal region? This would lead to an over-estimate of the background in the signal region and thus to a significant underestimate of the Higgs signal. Since the presently measured $H \rightarrow WW$ rates are indeed below SM expectations, for $m_H \approx 125$ GeV [2, 3], such scenario deserves serious investigation.

We will focus on processes arising within the Minimal Supersymmetric Standard Model (MSSM) as an example for processes induced by physics beyond the Standard Model (BSM physics). SUSY processes contributing as background have been discussed before with respect to calibration processes [4] and to Higgs boson searches within vector boson fusion where the Higgs boson decays into two tau leptons or two W bosons [5]. Also, in [6] SUSY processes as a possible background in the signal region of Higgs boson searches have been considered.

2 Scenario and analysis setup

Within the MSSM, processes that can contribute significantly to the signature of W boson pair production involve the production of charginos, sleptons and neutralinos and therefore the parameters that influence their masses are the most relevant ones.

Our scenario is based on the light slepton scenario described in [5], which is tuned for sizable chargino and slepton pair production. The tau slepton masses are chosen to be above the light chargino mass while the sleptons of the first two generations are lighter than the light chargino. As a consequence, the main decay channels of the charginos are via a slepton of the first two generations and a corresponding lepton, where the slepton decays directly into a lepton and the lightest neutralino (which is assumed to be the lightest supersymmetric particle (LSP)). We increase the chargino mass by modifying the soft SUSY

breaking parameters M_2 and m_{H_u} to be in agreement with the ATLAS 2 fb^{-1} trilepton search [7]. However our scenario shows strong tensions with the CMS trilepton analysis¹ [8] which uses the full 5 fb^{-1} dataset of 2011, if the predicted neutralino properties are taken literally. Since production processes with next-to-lightest neutralinos are not important for our analysis (see below), we ignore this tension having in mind alternative models that avoid the visible leptonic signature of the χ_2^0 .² The masses of squarks of the first two generations and of the gluino are not important for the following study and are set to high values. The parameters in the Higgs boson sector of the MSSM are assumed to have values which lead to a Standard Model type Higgs boson with mass of 124.7 GeV, which is within the experimentally allowed Higgs boson mass range and in the mass area where some experimental hints of a Higgs boson have been observed [9, 10]. Starting from this “base” scenario we vary the parameters that control the chargino, slepton and lightest neutralino masses to study their influence on the production and decay of the SUSY particles and their contribution to the W pair production signature. A scenario with 25% higher LSP and 40% higher slepton masses is discussed in more detail. The full parameter settings of the SUSY scenarios can be found in Appendix A. The following SUSY production processes give the dominant contributions to the signature of the W boson pair production:

$$q \bar{q} \rightarrow \chi_1^+ \chi_1^- \rightarrow \ell^+ \ell^- + \cancel{p}_T \quad (1)$$

$$q \bar{q} \rightarrow \tilde{\ell}^+ \tilde{\ell}^- \rightarrow \ell^+ \ell^- + \cancel{p}_T \quad (2)$$

$$q \bar{q} \rightarrow \chi_1^\pm \chi_2^0 \rightarrow \ell_1^+ \ell_2^+ \ell_2^- + \cancel{p}_T . \quad (3)$$

Chargino pair production gives the by far largest contribution, followed by the slepton pair production processes. The production of a next-to-lightest neutralino and a chargino gives only a very small contribution to the W boson pair production signature, as it produces mostly three leptons and the third lepton can be tagged quite well. Therefore this channel is not crucial for our results and general BSM scenarios without such a trilepton source can evade detection and still show the same behaviour concerning the WW background estimation.

It should be emphasized that the important feature of the scenarios is the existence of new physics particles which decay into electrons, muons and invisible particles, which is the same particle content in the final state as the one of the W pair production with subsequent leptonic decay. In that respect we consider our MSSM scenarios as an example for BSM physics.

The event generation for our analysis is done using **Herwig++** 2.5.2 [11] at parton level, including parton shower. Within **Herwig++**, the W pair production is generated at next-to-leading order QCD within the POWHEG framework [12]. The SUSY particle pairs are generated at leading order [13]. Their cross section is multiplied with an appropriate K-factor ($K = 1.2$), which we obtain from **Prospino2** [14]. Spin correlations within production and decay in **Herwig++** are included as described in [15]. A comparison with a combination of **MadGraph** 5.1.3 [16] and **Pythia** 6.4 [17] led to comparable results.

¹A possibility to weaken this tension is to allow a decay of the light chargino and the next-to-lightest neutralino into all three lepton flavors in equal parts. However this reduces the effect on the correction factor C by roughly 35-40%.

²This can be achieved for example with a scenario (typically beyond the MSSM) where the next-to-lightest neutralino is much heavier than the light chargino.

Both ATLAS [2] and CMS [3] have presented a study of the $H \rightarrow WW \rightarrow 2\ell 2\nu$ channel with the full data set of 2011. We largely use the cuts and methods from the ATLAS analysis, because they show distributions in the transverse mass of the W boson pair [18]

$$m_T = \sqrt{(E_T^{\ell\ell} + E_T^{miss})^2 - |\mathbf{p}_T^{\ell\ell} + \mathbf{p}_T^{miss}|^2}, \quad \text{with } E_T^{\ell\ell} = \sqrt{|\mathbf{p}_T^{\ell\ell}|^2 + m_{\ell\ell}^2}, \quad E_T^{miss} = |\mathbf{p}_T^{miss}| \quad (4)$$

in the signal and control regions up to quite high values in m_T . This gives an opportunity to check if the effects of BSM physics could be identified in the experiment as an excess of particularly hard events. CMS performs a similar analysis, but they only show distributions of the invariant lepton pair mass $m_{\ell\ell}$ and the azimuthal angle $\Delta\phi_{\ell\ell}$ between the leptons. Those distributions have turned out to be less illuminating for our study. However, as the CMS cut selection is similar to the ATLAS one, our results should hold qualitatively for CMS as well.

Our analysis is carried out for the LHC operating at a center-of-mass energy of 7 TeV. We use the CT10 parton distribution functions [19] for the POWHEG event samples and cteq611 pdfs for the leading order SUSY calculations. As renormalization and factorization scales we use the invariant mass of the W boson pair or the SUSY particle pair. For the basic event selection we require two oppositely charged leptons ℓ (electrons or muons), where the harder lepton with respect to transverse momentum p_T is labeled ℓ_1 , the softer one ℓ_2 . The following cuts are applied, largely taken from [2]:

$$\begin{aligned} p_{T,\ell_1} &> 25 \text{ GeV} & p_{T,\ell_2} &> 15 \text{ GeV} \\ m_{ee(\mu\mu)} &> 12 \text{ GeV} & m_{e\mu} &> 10 \text{ GeV} \\ |m_{ee(\mu\mu)} - M_Z| &> 15 \text{ GeV} & |\eta_\ell| &< 2.5 . \end{aligned} \quad (5)$$

The events are categorized according to the number of visible jets. Jets are clustered using the anti- k_t algorithm [20] with distance parameter $R = 0.4$ and the following requirements on rapidity η_j and $p_{T,j}$:

$$|\eta_j| < 4.5 \quad p_{T,j} > 25 \text{ GeV} . \quad (6)$$

Leptons that are within the R-separation $\Delta R < 0.3$ of a jet are counted as part of the jet. For QCD background suppression in the $H \rightarrow WW$ analysis the LHC experiments use the quantity $E_{T,rel}^{miss} = E_T^{miss} \cdot \sin \min(\Delta\phi, \frac{\pi}{2})$, where E_T^{miss} is the missing transverse energy of the event and $\Delta\phi$ is the azimuthal angle between the E_T^{miss} vector and the nearest lepton or jet with $p_T > 25 \text{ GeV}$. The requirement is

$$E_{T,rel}^{miss} > 45 \text{ GeV for } \ell\ell = ee(\mu\mu) \quad E_{T,rel}^{miss} > 25 \text{ GeV for } \ell\ell = e\mu . \quad (7)$$

The spin-0 nature of the Higgs boson is exploited by demanding [21]

$$\Delta\phi_{\ell\ell} < 1.8 . \quad (8)$$

The signal region in the 0-jet channel is furthermore restricted in the dilepton transverse momentum $p_T^{\ell\ell}$

$$p_T^{ee(\mu\mu)} > 45 \text{ GeV} \quad p_T^{e\mu} > 30 \text{ GeV} \quad (9)$$

and [22]

$$m_{\ell\ell} < 50 \text{ GeV} . \quad (10)$$

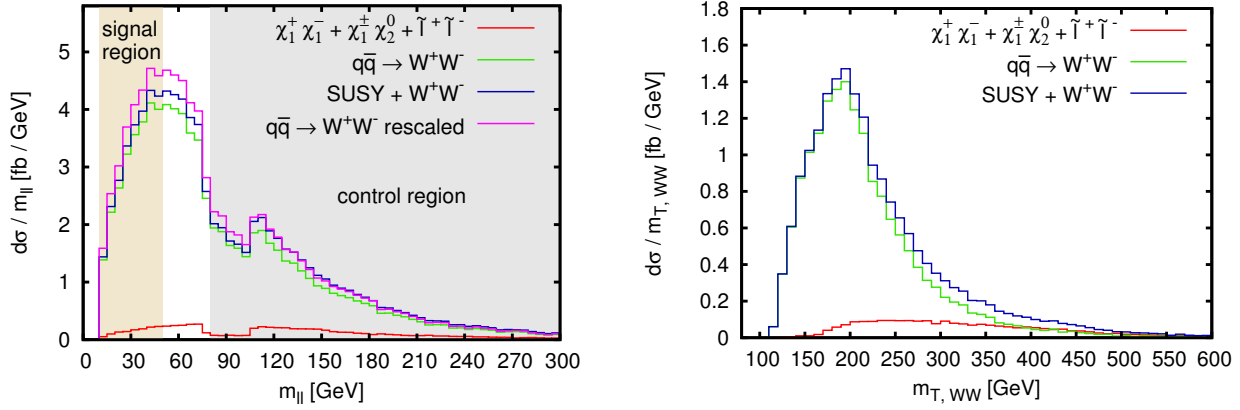


Figure 1: Invariant lepton pair mass $m_{\ell\ell}$ (left) and transverse mass m_T (right) distributions for the “base” scenario of Section 2. The m_T distribution is calculated including all control region cuts of Eqs. (5) - (7), (9) and (12). For the $m_{\ell\ell}$ plot the $m_{\ell\ell}$ -cut of Eq. (12) is omitted. Both plots show the $q\bar{q} \rightarrow WW$ distribution, the SUSY contributions and their sum. The $m_{\ell\ell}$ plot also shows the $q\bar{q} \rightarrow WW$ result, rescaled by $(\sigma_C^{WW} + \sigma_C^{SUSY})/\sigma_C^{WW}$, extracted from the control region.

For the 1-jet channel ATLAS uses cuts on the vectorial sum of the \mathbf{p}_T of jets, leptons and \mathbf{p}_T^{miss} , and on the $\tau\tau$ invariant mass $m_{\tau\tau}$, calculated in the collinear approximation [23]

$$|\mathbf{p}_T^{l_1} + \mathbf{p}_T^{l_2} + \mathbf{p}_T^j + \mathbf{p}_T^{miss}| < 30 \text{ GeV} \quad |m_{\tau\tau} - M_Z| > 25 \text{ GeV} . \quad (11)$$

Events with identified b-jets (80% efficiency, 6% mistag) are rejected. The WW control regions for the 0-jet and 1-jet bin are defined by omitting the $\Delta\phi_{\ell\ell}$ and $m_{\ell\ell, max}$ cuts of Eqs. (8) and (10) and requiring a minimal invariant lepton pair mass of

$$m_{\ell\ell} > 80 \text{ GeV} . \quad (12)$$

We do not consider the 2-jet channel, as there is not enough statistics at the moment for any conclusions in this channel. Detector effects, efficiencies and hadronization effects have been neglected.

3 Results for SUSY example

The effects of the SUSY processes of Eqs. (1) - (3) on the full $m_{\ell\ell}$ range (signal³ and control region) in the 0-jet channel can be seen in Figure 1. The situation for the 1-jet channel is very similar,⁴ but the BSM effects are much less constrained compared to the 0-jet channel due to smaller event numbers. Therefore we focus on the 0-jet bin. Chargino pair production accounts for the largest part of the SUSY signal, especially in the control region, while slepton pair production has larger effects in the low $m_{\ell\ell}$ region due to the small assumed

³The full signal region cuts also include a cut on $\Delta\phi_{\ell\ell}$, Eq. (8), but the effect on the WW and SUSY processes is marginal in the $m_{\ell\ell} < 50$ GeV region.

⁴Additional jets for the SUSY processes are simulated by the parton shower of Herwig++.

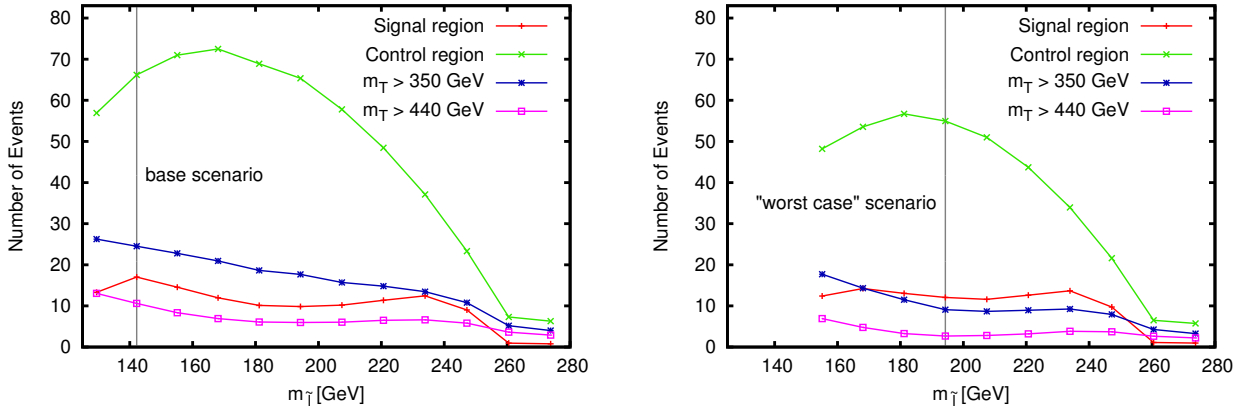


Figure 2: Event numbers of the SUSY contributions in the signal region, in the control region and in the control region with $m_T > 350$ GeV and $m_T > 440$ GeV for varying slepton masses of the first two generations. The LSP mass is $m_{\chi_1^0} = 99$ GeV in the left plot and $m_{\chi_1^0} = 124$ GeV in the right plot. The discussed “base” and “worst case” scenarios are marked.

slepton masses. As stated before, the production of a light chargino and the next-to-lightest neutralino has only a very small contribution and is therefore not important for our results. The relative contribution of the SUSY processes to the signal region is clearly much smaller than the contribution to the control region. Therefore this scenario is potentially dangerous for the data-driven estimation of the $q\bar{q} \rightarrow WW$ background: If the BSM physics could not be identified, the WW prediction in the signal region would be rescaled by

$$(\sigma_C^{WW} + \sigma_C^{SUSY})/\sigma_C^{WW}, \quad (13)$$

where σ_C^{WW} and σ_C^{SUSY} are the WW and BSM contributions in the control region. In our example, this leads to a WW prediction for the signal region which is clearly too high (see Figure 1). Furthermore the effect on the shape of the $m_{\ell\ell}$ and m_T distributions in the signal region is too small for a detection of the SUSY contamination.

In contrast, a closer look at the transverse mass distribution can reveal the BSM physics effects of this scenario. As m_T is bounded from below by $m_{\ell\ell}$ and additional missing transverse energy results in even larger values of m_T , BSM effects with large $m_{\ell\ell}$ naturally lead to contributions at high m_T values. This is especially the case in theories with additional sources of missing energy like the MSSM. Figure 1 shows an enhancement due to the SUSY contributions of more than 100% for m_T values exceeding 350-400 GeV. ATLAS measured 41 events with $m_T > 350$ GeV, with a total background expectation of 48 events, including a WW contribution of 31 events [2]. Therefore a factor of two increase in the “ WW contribution” is already ruled out with current data.

Most of the SUSY contributions arise from chargino pair production. As the masses of the chargino decay products play an important role for the kinematics of the final state leptons and for the amount of missing transverse momentum, we vary the soft SUSY breaking parameters M_1 , M_{eL} and $M_{\mu L}$, which govern the LSP and left-handed slepton masses. The slepton mass variation also directly modifies the slepton pair production contributions to signal and control region. For the identification of a potentially dangerous scenario (concerning

the normalization of the WW background with the help of a control region) the following constraints have to be fulfilled:

- The contribution to the signal region has to be as low as possible.
- The contribution to the control region has to be as large as possible, but still small enough to hide in the shape uncertainties of the control region.
- The part of the control region with high m_T is strongly constrained by the current ATLAS data. Therefore the BSM effect in this region has to be small.

For the comparison with the ATLAS data from [2], we convert our cross sections into expected number of events by normalizing our WW prediction for 4.7 fb^{-1} with the expected number of events from the ATLAS $H \rightarrow WW$ study within the 0-j control region. From this rescaling we estimate an overall efficiency of 59% for the evolution of showered parton level events to reconstructed jets and leptons in the analysis. For the rescaling we also take the $gg \rightarrow WW$ contribution into account using `gg2WW` [24], which is included in the $pp \rightarrow WW$ background of the ATLAS study. This part is formally of next-to-next-to leading order in QCD with respect to the $q\bar{q} \rightarrow WW$ contribution and adds a few percent to the cross section [1]. For the rest of our study, the $gg \rightarrow WW$ contribution has been neglected.

With this prescription the number of events shown in Figure 2 is calculated for a LSP mass of 99 GeV (left diagram) and 124 GeV (right diagram). For each plot the slepton mass is varied up to the chargino mass, bounded from below by the requirement that the lightest neutralino has to be the LSP. These event numbers have to be compared with the following values for the $q\bar{q} \rightarrow WW$ prediction (our Monte Carlo prediction, scaled with the overall efficiency factor 0.59):

$$N_{signal}^{WW} = 336 \quad N_{control}^{WW} = 454 \quad N_{m_T > 350 \text{ GeV}}^{WW} = 22 \quad N_{m_T > 440 \text{ GeV}}^{WW} = 7, \quad (14)$$

or $N_{m_T > 350 \text{ GeV}}^{WW} = 31$ and $N_{m_T > 440 \text{ GeV}}^{WW} = 11$ as taken from the ATLAS m_T distribution [2]. The discrepancy between those numbers can be ascribed to higher efficiencies for high m_T events. However, for our study we can largely eliminate this uncertainty by comparing ratios $N_{MC}^{SUSY} / N_{MC}^{WW}$ and the accuracy is sufficient for an approximate comparison with ATLAS data.

A slepton mass roughly in the middle between the LSP and chargino masses gives the largest contribution to the control region. At the same time, the tail of the m_T distribution is significantly smaller than for lighter sleptons. Furthermore the larger slepton mass shifts the slepton pair production contribution from the signal region to the control region. The increased LSP mass in the right plot of Figure 2 leads to less available kinetic energy for the decay products and therefore to smaller $m_{\ell\ell}$, m_T and p_T^{miss} . This further reduces the contributions in the high m_T bin of the control region. We also considered a larger chargino mass as input. This reduces the chargino pair production cross section and therefore leads to a reduction of the overall effect, as expected.

Taking the criteria as described above, we find a scenario which is compatible with the ATLAS $H \rightarrow WW$ analysis of 2011 data. We refer to it as the “worst case” scenario. As can be seen in Figures 2 and 3, this scenario gives very small contributions to the high m_T part of the control region, small enough so that they cannot be identified at the moment. At the

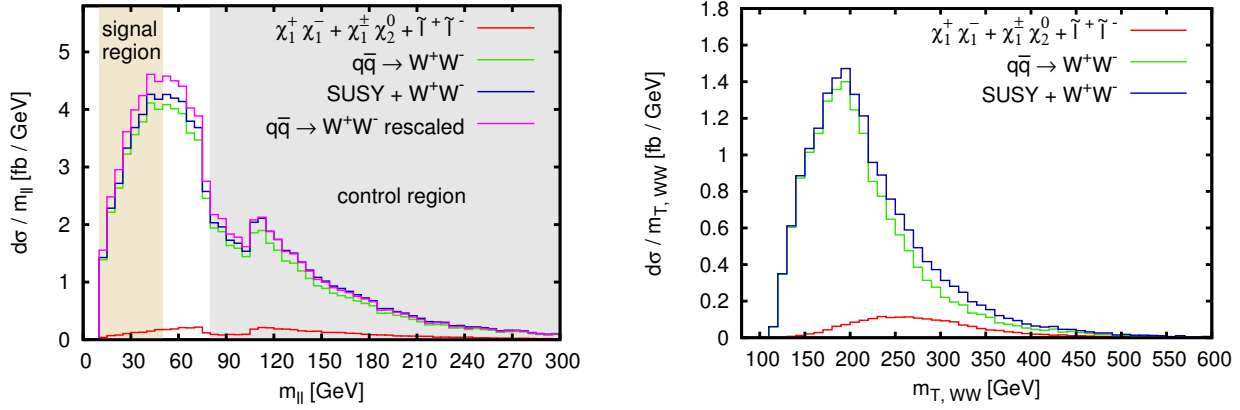


Figure 3: Invariant lepton pair mass $m_{\ell\ell}$ (left) and transverse mass m_T (right) distributions for the “**worst case**” scenario of Section 3. The m_T distribution is calculated including all control region cuts of Eqs. (5) - (7), (9) and (12). For the $m_{\ell\ell}$ plot the $m_{\ell\ell}$ -cut of Eq. (12) is omitted. Both plots show the $q\bar{q} \rightarrow WW$ distribution, the SUSY contributions and their sum. The $m_{\ell\ell}$ plot also shows the $q\bar{q} \rightarrow WW$ result, rescaled by $(\sigma_C^{WW} + \sigma_C^{SUSY})/\sigma_C^{WW}$, extracted from the control region.

same time the contributions to the signal region are very small and therefore not noticeable, although they are at partially higher values of m_T than the WW background.

We now want to quantify the effect of this BSM scenario on the WW background prediction calculating the factor C by which the expected number of WW events in the signal region obtained from the normalization would have to be corrected. The extrapolation for the number of events from control to signal region is done using [1]

$$N_S = \frac{N_{S,MC}^{WW}}{N_{C,MC}^{WW}} N_C = \alpha \cdot N_C. \quad (15)$$

Taking both Standard Model WW production and the BSM effects in the control region into account, this leads to a predicted number of background events in the signal region given by

$$N_S^{norm} = \alpha \cdot (N_C^{WW} + N_C^{SUSY}), \quad (16)$$

while the actual contribution is

$$N_S^{true} = N_S^{WW} + N_S^{SUSY}. \quad (17)$$

Therefore the predicted number of events would have to be reduced by

$$C = \frac{N_S^{true}}{N_S^{norm}} = \frac{\sigma_S^{WW} + \sigma_S^{SUSY}}{\sigma_C^{WW} + \sigma_C^{SUSY}} \cdot \frac{\sigma_C^{WW}}{\sigma_S^{WW}} \quad (18)$$

where we have replaced ratios of event numbers by our theoretical cross sections. For this specific scenario we get

$$C = 0.924. \quad (19)$$

For the ATLAS data which enters their fitting procedure and the resulting exclusion limits a selection cut of

$$0.75 \cdot m_H < m_T < m_H \quad (20)$$

on the transverse mass is applied. Within this range the relative BSM contribution of our “worst case” scenario is even smaller, leading to a larger correction for the extraction of the WW background. In this case the number of WW events would have to be reduced by a factor of

$$C = 0.897. \quad (21)$$

Since a SM Higgs signal is about 20% of the overall background, an overestimate of 10% in the (dominant) WW background would lead to a very large underestimate in the size of the extracted Higgs signal.

4 Conclusions

Data driven methods for background determination are extremely useful for reducing theory errors inherent in QCD predictions for LHC cross sections. However, they do rely on assumptions, namely that, apart from the searched signal events, there are no other BSM contributions which could affect the search. In this paper we have studied the impact of new physics contributions on the estimate of the SM background to the $H \rightarrow WW \rightarrow \ell\bar{\nu}\ell\nu$ search. In the case of W pair production as background to Higgs boson searches, the number of events is measured in a high $m_{\ell\ell}$ control region where no signal events are to be expected. Via an extrapolation using Monte Carlo predictions for the SM-shape of the distributions of W pair production, the estimate of the background in the softer signal region is determined. In general, new physics at high energy scales can enhance the number of events in hard control regions while contributing little to a substantially softer signal region. The larger measured rate in the control region then can lead to an overestimate of the background in the signal region and dilute a potential signal.

Two example scenarios in the context of the MSSM have been discussed in some detail. In the first one, the new physics contributions not only lead to an enhancement of the event rates in the control region but also change the shape of distributions (the m_T distribution in the case considered) sufficiently to make the extra BSM contributions noticeable. The new physics contributions in the second example are more difficult to distinguish from the pure SM case and could indeed have been missed in the $H \rightarrow WW$ analyses. With enough data, one could, of course, see deviations in the hard event distributions, like in the tail of m_T distributions for the scenarios at hand.

The MSSM scenario described above is just one example of BSM physics which might affect the Higgs search and, as importantly, the measurement of Higgs couplings from measured Higgs rates. Such potential BSM contamination should be kept in mind when interpreting the Higgs search data within BSM scenarios: the errors on Higgs boson couplings may be larger than in a pure SM analysis.

Acknowledgments

We would like to thank Stefan Gieseke, Keith Hamilton and Christian Röhr for discussions and Herwig++ support. We gratefully acknowledge helpful discussions with Sophy Palmer, Eva Popenda and Michael Rauch. This work was supported by the BMBF under Grant No. 05H09VKG (“Verbundprojekt HEP-Theorie”) and by the Initiative and Networking Fund of the Helmholtz Association, contract HA-101 (“Physics at the Terascale”).

A Parameters

The “base” scenario is determined by the soft SUSY breaking parameters

$$\begin{aligned}
 M_1 &= 103.1 \text{ GeV} & M_{eL} = M_{\mu L} &= 134.4 \text{ GeV} \\
 M_2 &= 270.1 \text{ GeV} & M_{eR} = M_{\mu R} &= 135.8 \text{ GeV} \\
 M_3 &= 1703.7 \text{ GeV} & M_{\tau L} &= 393.6 \text{ GeV} \\
 A_t &= -2194.8 \text{ GeV} & M_{\tau R} &= 333.4 \text{ GeV} \\
 A_b &= -1907.2 \text{ GeV} & M_{q_1 L} = M_{q_2 L} &= 1579.8 \text{ GeV} \\
 A_\tau &= -249.4 \text{ GeV} & M_{uR} = M_{cR} &= 1524.3 \text{ GeV} \\
 A_u = A_c &= -655.5 \text{ GeV} & M_{dR} = M_{sR} &= 1517.7 \text{ GeV} \\
 A_d = A_s &= -821.8 \text{ GeV} & M_{q_3 L} &= 1201.4 \text{ GeV} \\
 A_e = A_\mu &= -251.1 \text{ GeV} & M_{tR} &= 1019.4 \text{ GeV} \\
 M_{H_d}^2 &= 32609 \text{ GeV}^2 & M_{bR} &= 1257.2 \text{ GeV} \\
 M_{H_u}^2 &= -169877 \text{ GeV}^2 & \tan \beta(M_Z) &= 10.0
 \end{aligned} \tag{22}$$

at the scale $Q = 1 \text{ TeV}$ and the following Standard Model parameters, with the top mass from [25]:

$$\begin{aligned}
 \alpha_{em}^{-1}(M_Z) &= 127.934 & G_F &= 1.16639 \cdot 10^{-5} \text{ GeV}^{-2} \\
 \alpha_s(M_Z) &= 0.1172 & M_Z &= 91.187 \text{ GeV} \\
 M_b(M_b) &= 4.25 \text{ GeV} & M_t &= 173.2 \text{ GeV} .
 \end{aligned} \tag{23}$$

These parameters are fed into SUSYHIT [26] for the calculation of the SUSY particle masses and branching ratios. The SLHA output file is then used as input for FeynHiggs 2.8.6 [27] in order to get precise Higgs boson mass values. The resulting scenario exhibits the following features:

- The squark mass values of all three generations and the gluino mass values ($m_{\tilde{q}} \approx 1581 \text{ GeV}$, $m_{\tilde{t}_1} = 934 \text{ GeV}$, $m_{\tilde{b}_1} = 1232 \text{ GeV}$, $m_{\tilde{g}} = 1725 \text{ GeV}$) are beyond current exclusion limits [28–31].
- The trilinear coupling A_t is adjusted according to the maximal mixing scenario [32], which yields a Higgs boson mass with values in the vicinity of the experimental hints of a Higgs boson [9, 10].
- The wino mass parameter M_2 and the Higgs mass parameter m_{H_u} are chosen to give chargino masses outside the exclusion limits of the ATLAS trilepton search [7]. The discussion of the 5 fb^{-1} CMS trilepton analysis [8] can be found in Section 2.

	“base” scenario	“worst case” scenario
	$M_{e,\mu L,R} = M_{e,\mu L,R}^0$ $M_1 = 103 \text{ GeV}$	$M_{e,\mu L,R} = 1.4 \cdot M_{e,\mu L,R}^0$ $M_1 = 129 \text{ GeV}$
$m_{\chi_1^0}$	98.9 GeV	124.1 GeV
$m_{\chi_1^+}$	260.0 GeV	260.3 GeV
$m_{\chi_2^0}$	260.3 GeV	260.7 GeV
$m_{\tilde{e}_L} = m_{\tilde{\mu}_L}$	141.8 GeV	193.5 GeV
$m_{\tilde{e}_R} = m_{\tilde{\mu}_R}$	142.6 GeV	195.0 GeV
$BR(\chi_1^+ \rightarrow \ell^+ \tilde{\nu}_\ell)$	58.0 %	60.4 %
$BR(\chi_1^+ \rightarrow \tilde{\ell}_L^+ \nu_\ell)$	41.0 %	37.7 %
$BR(\chi_1^+ \rightarrow W^+ \chi_1^0)$	1.0 %	1.9 %
$BR(\chi_2^0 \rightarrow \tilde{\ell}_{L,R}^\pm \ell^\mp)$	47.7 %	45.1 %
$BR(\chi_2^0 \rightarrow \tilde{\nu}_\ell \bar{\nu}_\ell)$	51.4 %	53.2 %
$BR(\chi_2^0 \rightarrow \chi_1^0 Z)$	0.2 %	0.3 %
$BR(\chi_2^0 \rightarrow \chi_1^0 h_0)$	0.7 %	1.4 %
$BR(\tilde{\ell}_{L,R}^\pm \rightarrow \chi_1^0 \ell^\pm)$	100.0%	100.0%

Table 1: Masses and branching ratios of interest for our “base” scenario and for a scenario with modified M_1 and $M_{e,\mu L,R}$. Here, $\tilde{\ell}$ means the combined (s)electron and (s)muon channel. For completeness, we also give the mass and the branching ratios of the χ_2^0 though they are not important for our results.

- The stau lepton masses are larger than the light chargino mass ($m_{\tilde{\tau}_1} = 334 \text{ GeV}$), which is a specific feature of the considered scenarios.
- The mass parameters for the left-handed sleptons of the first two generations M_{eL} and $M_{\mu L}$ are chosen such that the chargino decay into selectrons and smuons is the dominant decay mode.

The soft SUSY breaking parameters of the “worst case” scenario discussed in Section 3 are the same as in the “base” scenario, except for

$$\begin{aligned}
M_1 &= 128.9 \text{ GeV} & M_{eR} = M_{\mu R} &= 190.1 \text{ GeV} \\
M_{eL} = M_{\mu L} &= 188.2 \text{ GeV} .
\end{aligned} \tag{24}$$

The relevant masses and branching ratios of both scenarios are listed in Table 1.

References

- [1] LHC Higgs Cross Section Working Group, CERN-2012-002 (CERN, Geneva, 2012) , [arXiv:1201.3084 \[hep-ph\]](https://arxiv.org/abs/1201.3084).

- [2] **ATLAS Collaboration**, ATLAS-CONF-2012-012, CERN, Geneva, Mar, 2012.
- [3] **CMS Collaboration**, S. Chatrchyan *et al.*, [arXiv:1202.1489 \[hep-ex\]](#).
- [4] H. Baer, V. Barger and G. Shaughnessy, *Phys.Rev.* **D78** (2008) 095009, [arXiv:0806.3745 \[hep-ph\]](#).
- [5] B. Feigl, H. Rzehak and D. Zeppenfeld, *Eur.Phys.J.* **C72** (2012) 1903, [arXiv:1108.1110 \[hep-ph\]](#).
- [6] M. Lisanti and N. Weiner, [arXiv:1112.4834 \[hep-ph\]](#).
- [7] **ATLAS Collaboration**, G. Aad *et al.*, [arXiv:1204.5638 \[hep-ex\]](#).
- [8] **CMS Collaboration**, S. Chatrchyan *et al.*, [arXiv:1204.5341 \[hep-ex\]](#); **CMS Collaboration**, CMS-PAS-SUS-11-016, (2012).
- [9] **ATLAS Collaboration**, G. Aad *et al.*, *Phys.Lett.* **B710** (2012) 49–66, [arXiv:1202.1408 \[hep-ex\]](#); **ATLAS Collaboration**, ATLAS-CONF-2012-019, CERN, Geneva, Mar, 2012.
- [10] **CMS Collaboration**, S. Chatrchyan *et al.*, [arXiv:1202.1488 \[hep-ex\]](#); **CMS Collaboration**, CMS-PAS-HIG-12-008, (2012).
- [11] M. Bahr *et al.*, *Eur.Phys.J.* **C58** (2008) 639–707, [arXiv:0803.0883 \[hep-ph\]](#); S. Gieseke *et al.*, [arXiv:1102.1672 \[hep-ph\]](#).
- [12] K. Hamilton, *JHEP* **1101** (2011) 009, [arXiv:1009.5391 \[hep-ph\]](#).
- [13] M. Gigg and P. Richardson, *Eur.Phys.J.* **C51** (2007) 989–1008, [arXiv:hep-ph/0703199](#); M. Gigg and P. Richardson, [arXiv:0805.3037 \[hep-ph\]](#).
- [14] W. Beenakker, M. Klasen, M. Kramer, T. Plehn, M. Spira and P. Zerwas, *Phys.Rev.Lett.* **83** (1999) 3780–3783, [arXiv:hep-ph/9906298](#).
- [15] P. Richardson, *JHEP* **0111** (2001) 029, [arXiv:hep-ph/0110108](#).
- [16] J. Alwall, M. Herquet, F. Maltoni, O. Mattelaer and T. Stelzer, *JHEP* **1106** (2011) 128, [arXiv:1106.0522 \[hep-ph\]](#); J. Alwall *et al.*, *JHEP* **0709** (2007) 028, [arXiv:0706.2334 \[hep-ph\]](#); J. Alwall *et al.*, *AIP Conf. Proc.* **1078** (2009) 84–89, [arXiv:0809.2410 \[hep-ph\]](#).
- [17] T. Sjostrand, S. Mrenna and P. Z. Skands, *JHEP* **0605** (2006) 026, [arXiv:hep-ph/0603175](#).
- [18] A. J. Barr, B. Gripaios and C. G. Lester, *JHEP* **0907** (2009) 072, [arXiv:0902.4864 \[hep-ph\]](#).
- [19] H.-L. Lai *et al.*, *Phys. Rev.* **D82** (2010) 074024, [arXiv:1007.2241 \[hep-ph\]](#).

- [20] M. Cacciari, G. P. Salam and G. Soyez, *JHEP* **0804** (2008) 063, [arXiv:0802.1189 \[hep-ph\]](#).
- [21] M. Dittmar and H. Dreiner, *Phys.Rev.* **D55** (1997) 167–172, [arXiv:hep-ph/9608317](#).
- [22] V. Barger, G. Bhattacharya, T. Han and B. Kniehl, *Phys.Rev.* **D43** (1991) 779–788.
- [23] R. K. Ellis, I. Hinchliffe, M. Soldate and J. J. V. D. Bij, *Nuclear Physics B* **297** (1988) 221 – 243.
- [24] T. Binoth, M. Ciccolini, N. Kauer and M. Kramer, *JHEP* **0503** (2005) 065, [arXiv:hep-ph/0503094](#);
T. Binoth, M. Ciccolini, N. Kauer and M. Kramer, *JHEP* **0612** (2006) 046, [arXiv:hep-ph/0611170](#).
- [25] **Tevatron Electroweak Working Group, for the CDF and D0 Collaborations**, [arXiv:1107.5255 \[hep-ex\]](#).
- [26] A. Djouadi, M. M. Muhlleitner and M. Spira, *Acta Phys.Polon.* **B38** (2007) 635–644, [arXiv:hep-ph/0609292](#);
A. Djouadi, J.-L. Kneur and G. Moultaka, *Comput.Phys.Commun.* **176** (2007) 426–455, [arXiv:hep-ph/0211331](#);
M. Muhlleitner, A. Djouadi and Y. Mambrini, *Comput.Phys.Commun.* **168** (2005) 46–70, [arXiv:hep-ph/0311167](#);
A. Djouadi, J. Kalinowski and M. Spira, *Comput.Phys.Commun.* **108** (1998) 56–74, [arXiv:hep-ph/9704448](#).
- [27] S. Heinemeyer, W. Hollik and G. Weiglein, *Comput.Phys.Commun.* **124** (2000) 76–89, [arXiv:hep-ph/9812320](#);
S. Heinemeyer, W. Hollik and G. Weiglein, *Eur.Phys.J.* **C9** (1999) 343–366, [arXiv:hep-ph/9812472](#);
G. Degrassi, S. Heinemeyer, W. Hollik, P. Slavich and G. Weiglein, *Eur.Phys.J.* **C28** (2003) 133–143, [arXiv:hep-ph/0212020](#);
M. Frank, T. Hahn, S. Heinemeyer, W. Hollik, H. Rzehak and G. Weiglein, *JHEP* **0702** (2007) 047, [arXiv:hep-ph/0611326](#).
- [28] **ATLAS Collaboration**, G. Aad *et al.*, *Phys.Lett.* **B710** (2012) 67–85, [arXiv:1109.6572 \[hep-ex\]](#);
ATLAS Collaboration, ATLAS-CONF-2012-033, CERN, Geneva, Mar, 2012.
- [29] **CMS Collaboration**, S. Chatrchyan *et al.*, *Phys.Rev.Lett.* **107** (2011) 221804, [arXiv:1109.2352 \[hep-ex\]](#);
CMS Collaboration, CMS-PAS-SUS-12-005, (2012).
- [30] **ATLAS Collaboration**, [arXiv:1204.6736 \[hep-ex\]](#).
- [31] **ATLAS Collaboration**, G. Aad *et al.*, [arXiv:1112.3832 \[hep-ex\]](#).
- [32] M. S. Carena, S. Heinemeyer, C. E. M. Wagner and G. Weiglein, [arXiv:hep-ph/9912223](#).